



Gluon Exchange Corrections to the Nucleon Magnetic Moment in the MIT Bag Model

A. HALPRIN^{*} and P. SORBA^{†‡}

Fermi National Accelerator Laboratory^{**}, Batavia, Illinois 60510

ABSTRACT

We have calculated gluon exchange corrections to the nucleon magnetic moment predictions of the MIT bag model. The sizeable coupling constant $\frac{g_c^2}{4\pi} = 0.5$ does not produce an enormous correction ($\sim 10\%$), but it is in the wrong direction to ameliorate the present 30% disagreement with experiment.

^{*}Permanent address University of Delaware, Newark, Delaware 19711

[†]On leave of absence from Centre de Physique Theorique, CNRS, Marseille, France.

[‡]Work supported in part by the National Science Foundation.

The MIT bag model has enjoyed a certain measure of success in describing the low lying hadron spectrum.¹⁻³ Since it is a complete dynamical model, in contrast to a group theoretical model, it is capable of predicting the absolute values of hadron magnetic moments. These moments are especially interesting, because they involve no recoil and do not force us to deal with an empty bag, in contrast to other transition currents.^{4, 5} One would expect the rigid spherical cavity approximation used thus far to be inadequate for states of high excitation, and we shall limit ourselves to the proton and neutron magnetic moments. The ratio of neutron to proton moments is the standard SU_6 value of $-2/3$, but the present prediction for the proton magnetic moment is 30% below the experimental value. As remarked by DeGrand et al., this rather serious discrepancy can hopefully be accounted for by higher order corrections.³

In the case of QED, second order photon exchange corrections increase the positron magnetic moment over the Dirac value, and one might analogously expect a substantial increase in the proton moment due to second order gluon exchange effects. However, as we have discussed in the case of a related vertex correction, confinement has a violent effect on naive free particle Feynman diagrams and may even change their sign.⁶ We have calculated all second order gluon exchange diagrams associated with the lowest energy quark eigenmode within the framework of the static capability approximation. The proton moment

is reduced from the zero order result by 10%, which therefore exacerbates the existing discrepancy.

As in our previous work, we utilize old fashioned stationary state perturbation theory and employ the radiation gauge for the gluon field.^{6,7} The nonabelian character of the gluon field is of no consequence to this order and the quark-gluon interaction Hamiltonian can be written as

$$H_S = H_1 + H_2 \quad (1)$$

$$H_1 = - (4\pi\alpha_c)^{\frac{1}{2}} \int \bar{\psi}(x) \vec{\gamma} \cdot \lambda^{\ell} \psi(x) \cdot \vec{A}_{\ell}(x) d^3x \quad (2)$$

$$H_2 = \frac{\alpha_c}{2} \int \frac{\psi(x)^+ \lambda^{\ell} \psi(x) \psi(y)^+ \lambda_{\ell} \psi(y)}{|\vec{x} - \vec{y}|} d^3x d^3y, \quad (3)$$

where λ^{ℓ} are the color SU_3 matrices and $\alpha_c = 0.5$. The relevant electromagnetic interaction is the quark-magnetic field coupling,

$$H_m = - \frac{1}{2} \int \left[\vec{r} \times \bar{\psi}(r) \vec{\gamma} \psi(r) \right]_3 B. \quad (4)$$

where B is the third component of the external magnetic field.

Our starting point for the correction to the magnetic moment of the nucleon, \mathcal{N} , is

$$\delta\mu = - \left. \frac{\partial \langle \mathcal{N} | H | \mathcal{N} \rangle}{\partial B} \right|_{B=0}. \quad (5)$$

To second order in H_S ,

$$\begin{aligned} \delta\mu = & \langle \mathcal{N}_0 | H_S G^+ H_m B^{-1} G H_S | \mathcal{N}_0 \rangle \\ & - \langle \mathcal{N}_0 | H_m B^{-1} | \mathcal{N}_0 \rangle \langle \mathcal{N}_0 | H_S G^+ G | H_S | \mathcal{N}_0 \rangle \end{aligned} \quad (6)$$

$$G = (E_{\mathcal{N}} - H_0)^{-1} \left(1 - |\mathcal{N}_0\rangle \langle \mathcal{N}_0| \right). \quad (7)$$

$|\mathcal{N}_0\rangle$ is the static up-spin nucleon state to zero order in H_S . To first order in α_c we must consider the diagrams shown in Fig. 1. Diagrams involving H_2 are absent owing to a cancellation between two quark correlations and single quark self-interactions induced by H_2 . This is similar to the absence of electrostatic terms in the nucleon energies calculated in Reference 3. We also drop all other diagrams that differ from the zero order α_c result by self-energy insertions under the assumption that they are properly accounted for by using renormalized masses.

For $H_S = H_m = 0$, the cavity approximation to the classical quark field must satisfy the free Dirac equation and the linear boundary condition

$$-i \vec{r} \cdot \vec{\gamma} \psi(\vec{r}, t) = \psi(\vec{r}, t), \quad (8)$$

on the sphere $r = R$. The results appear to be insensitive to the u and d quark mass values, and we will set them equal to zero. The Dirac equation and Eq. (8) then imply the eigenvalue equations

$$j_{j - \frac{1}{2}}(ER) = (-1)^{j - \frac{1}{2} + \ell} = j_{j + \frac{1}{2}}(ER), \quad (9)$$

where $j_m(ER)$ is the spherical Bessel function regular at the origin, j is the total quark angular momentum, and the parity of the state is $(-1)^\ell$, $\ell = j \pm \frac{1}{2}$. Inspection of Bessel function tables shows that the three lowest positive energy modes are $S_{1/2}$, $P_{3/2}$ and $P_{1/2}$ states with $ER = 2.0, 3.2, 3.8$ and parity $1, -1, -1$, respectively. The corresponding antiparticles have opposite parity, i.e. they are $P_{1/2}$, $D_{3/2}$ and $S_{1/2}$ states, respectively.

The classical bag model also imposes a quadratic boundary condition that determines the bag radius in terms of the other parameters of the theory. To zero order in α_c it only allows one quark field mode and its antiparticle mode to be excited in a given bag. Extension to the quantum domain is ambiguous, particularly with regard to virtual states.⁸ For the purpose of this calculation we restrict the intermediate state quarks to be in the same mode as those of the nucleon bag, which is the lowest $S_{1/2}$ mode, and we restrict intermediate state antiquarks to the $P_{1/2}$ mode of the same energy.

We therefore need only consider diagrams (a) and (b) of Fig. 1, since in all other diagrams a different gluon parity assignment is required at each of the two strong vertices. In the surviving diagrams parity and angular momentum, require the gluon to be in a unit angular momentum, transverse electric (TE) mode. Antiquarks do not enter, and the required wavefunction associated with destruction of the $S_{1/2}$ quark is

$$q_\ell(\vec{r}) = \frac{N}{4\pi} \begin{pmatrix} i j_0(ER) U_\ell \\ -j_1(ER) \vec{\sigma} \cdot \hat{r} U_\ell \end{pmatrix} \quad (10)$$

$$N^{-2} = 2R^3 j_0(ER)^3 (ER - 1) (ER)^{-1} . \quad (11)$$

U_ℓ is a 2-spinor and $ER = 2.0$. The transverse gluon field must satisfy the boundary conditions

$$\hat{r} \cdot \vec{A}^a = 0, \quad \vec{\nabla} \times \vec{\nabla} \times \vec{A}^a = 0 \quad \text{on } r = R . \quad (12)$$

The required unit angular momentum gluon wavefunction is

$$G_{mn}(\vec{r}) = N_{mn} \left[i_m \hat{\theta} - (|m| \cos \theta - \delta_{m0} \sin \theta) \hat{\phi} \right] j_1(k_n r) \quad (13)$$

$$N_{mn}^{-2} = 2 k_m \frac{4\pi}{3} (1 + |m|) \left[j_1(k_n R)^2 - j_0(k_n R) j_2(k_n R) \right], \quad (14)$$

where $k_n R = 2.7, 6.1, 9.11, \dots$ is determined by

$$\frac{d \left[k_n R j_1(k_n R) \right]}{d(k_n R)} = 0 . \quad (15)$$

The contribution from diagram (a) can be written as

$$\delta\mu_a = 4\pi\alpha_c \mu_0 \langle \mathcal{N}_0 | \sum_i (\sigma_3 Q)_i \sum_n k_n^{-2} A_n | \mathcal{N}_0 \rangle, \quad (16)$$

where $\mu_0 \langle \mathcal{N}_0 | \sum_i (\sigma_3 Q)_i | \mathcal{N}_0 \rangle$ is the magnetic moment to zero order in α_c , $1/2 \sigma_{3i}$ and Q_i are the spin and charge operators for the i th quark, and A_n is defined through

$$\begin{aligned} A_n U_F^+ \sigma_3 U_I = & \langle \mathcal{N}_0 | \int d^3x \vec{G}_{mn}(x) \cdot \bar{q}_F(x) \vec{\gamma} \lambda^a q_t(x) U_t^+ \sigma_3 \\ & \times U_t \int d^3y \bar{q}_t(y) \vec{\gamma} \lambda_a q_I(y) \cdot \vec{G}_{mn}(y)^* | \mathcal{N} \rangle. \end{aligned} \quad (17)$$

The contribution from diagram b is given by

$$\delta\mu_b = 4\pi\alpha_c \mu_0 \langle \mathcal{N}_0 | \sum_{i \neq j} \left(\{ \sigma_3, \sigma^\ell \} + Q \right)_i (\sigma_\ell)_j \sum_n k_n^{-2} b_n | \mathcal{N}_0 \rangle, \quad (18)$$

where b_n is defined through

$$\begin{aligned} b_n \left(U_F^+ \{ \sigma_3, \sigma^\ell \} + U_I \right)_i \left(U_F^+ \sigma_\ell U_I \right)_j = \\ \int d^3x \vec{G}_{mn}(x) \cdot \left(\bar{q}_F(x) \lambda^a \{ \sigma_3, \vec{\gamma} \} + q_I(x) \right)_i \int d^3y \left(\bar{q}_F(y) \lambda_a \vec{\gamma} q_I(y) \right)_j \cdot \vec{G}_{mn}^*(y). \end{aligned} \quad (19)$$

The angular integrations and gluon spin sums are tedious but straightforward and we will not bore the reader with these details. Utilizing

the relation $\lambda^a \lambda_a = 16/3$ and the fact that the color singlet character of the nucleon state allows us to let $\lambda_i^a \lambda_{aj} \rightarrow -8/3$ for $i \neq j$, we obtain

$$A_n = 2b_n = -\frac{16}{3} \left(\frac{4}{3}\right)^2 \left(\frac{N^2 N_{0n}}{E^3}\right)^2 I_n^2, \quad (20)$$

where

$$I_n = \int_0^{2.0} j_0(y) j_1(y) j_1\left(\frac{k_n}{E} y\right) dy. \quad (21)$$

The numerical values of I_n are given in Table 1, and it is clear that $n > 1$ gluon modes contribute less than 1%. We also note that

$$\sum_{i \neq j} \left(Q \{ \sigma_3, \sigma^{\ell} \}_+ \right)_i (\sigma^{\ell})_j = 2 \left[\sum_i (\sigma_3)_i \sum_i Q_i - \sum_i (\sigma_3 Q)_i \right]. \quad (22)$$

Our final result for diagrams (a) and (b) taken together is therefore proportional to the total nucleon charge. Completing the numerics, the neutron and proton moment corrections are

$$\delta \mu_n = 0 \quad (23)$$

$$\delta \mu_p = -0.1 \mu_p^{(0)}, \quad (24)$$

where $\mu_p^{(0)}$ is the proton moment of DeGrand et al., and we have used $\langle \text{proton} | \sum_i (\sigma_3 Q)_i | \text{proton} \rangle = 1.$ ⁹

Conclusions:

Gluon exchange corrections cannot account for the 30% discrepancy between experiment and the bag model prediction for the proton magnetic moment and give a 10% correction in the wrong direction. It is doubtful that the model parameters can be adjusted enough to resolve this discrepancy without grossly mucking up the fit to the mass spectrum. Perhaps boundary fluctuations can have a large influence on the static properties of even the lowest hadron states, but that remains to be seen.¹⁰ However, the corrections are not overwhelmingly large, which lends a degree of credibility to the use of perturbation theory when the coupling constant is so close to unity, i. e. : $\frac{g_c^2}{4\pi} = 0.5$.

ACKNOWLEDGMENT

The authors would like to thank R. Pearson for numerical assistance, and M. Barnhill and V. Matveev for helpful conversations. We should also like to thank B. W. Lee for his kind hospitality at the Fermilab Theory Department.

FOOTNOTES AND REFERENCES

- ¹A. Chodos, R.L. Jaffe, K. Johnson, C.B. Thorn, and V.F. Weisskopf, Phys. Rev. D9, 3471 (1974).
- ²A. Chodos, R.L. Jaffe, K. Johnson, and C.B. Thorn, Phys. Rev. D10, 2599 (1974).
- ³T. DeGrand, R.L. Jaffe, K. Johnson, and J. Kiskis, Phys. Rev. D12, 2060 (1975).
- ⁴J. F. Donoghue, E. Golowich, and B. R. Holstein, Phys. Rev. D12, 2875 (1975).
- ⁵P. Hays and V. K. Ulehla, Phys. Rev. D13, 1339 (1975).
- ⁶A. Halprin, B. W. Lee, and P. Sorba, (to be published in Phys. Rev.).
- ⁷The linear bag model boundary condition for the gluon field does allow one to pass from the interaction $-g_c \bar{\psi} \gamma_\mu \lambda^k \psi A_k^\mu$ to that given in Eq. (1) ($\alpha_c = g_c^2/4\pi$).
- ⁸For discussions of this point see Ref. 4 and T. A. DeGrand and R. L. Jaffe, MIT preprint # 529.
- ⁹R. van Royen and V. F. Weisskopf, II Nuovo Cimento, LA, 617 (1967).
- ¹⁰C. Rebbi, Phys. Rev. D12, 1407 (1975).

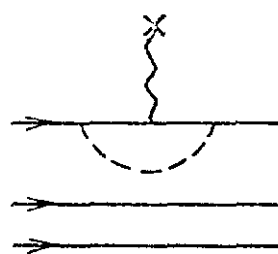
FIGURE AND TABLE CAPTIONS

Fig. 1: Non-covariant perturbation diagrams for the nucleon magnetic moment. The solid, dotted and wavy lines represent quark, gluon and magnetic field photon, respectively. A lightning stroke is a quark-antiquark pair.

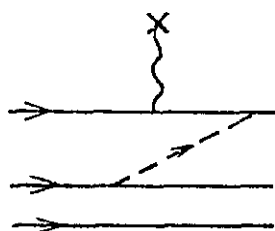
Table 1: Numerical values of the integral I_n of Eq. (21).

n	1	2	3
I_n	0.261	0.010	-0.002

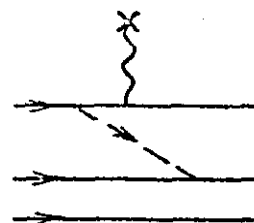
Table 1



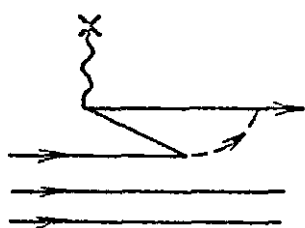
(a)



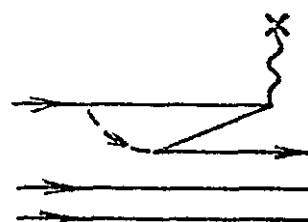
(b₁)



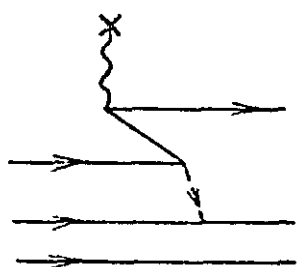
(b₂)



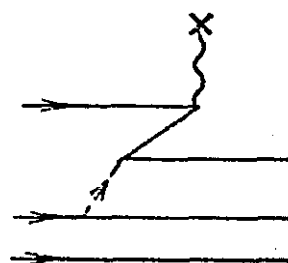
(c₁)



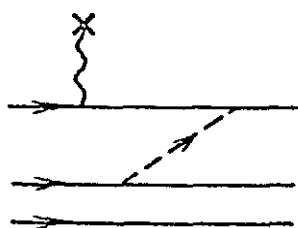
(c₂)



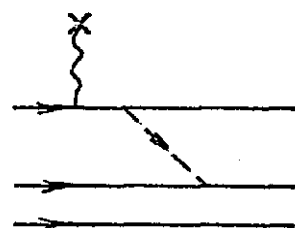
(d₁)



(d₂)



(e₁)



(e₂)